JOURNAL OF AGRICULTURAL AND FOOD CHEMISTRY
ARTICLE

J. Agric. Food Chem. 2010, 58, 12547–12556 12547
DOI:10.1021/jf103159r

# Tricetin, a Dietary Flavonoid, Induces Apoptosis through the Reactive Oxygen Species/c-Jun $NH_2$-Terminal Kinase Pathway in Human Liver Cancer Cells

Ya-Ling Hsu,[†] Ming-Feng Hou,[‡,§] Eing-Mei Tsai,[†,#,⊥] and Po-Lin Kuo*[,†,‡,§,⊥,⊗]

[†]Graduate Institute of Medicine, College of Medicine, Kaohsiung Medical University, No. 100 Shih-Chuan First Road, Kaohsiung 807, Taiwan, [‡]Institute of Clinical Medicine, College of Medicine, Kaohsiung Medical University, No. 100 Shih-Chuan First Road, Kaohsiung 807, Taiwan, [§]Cancer Center, Kaohsiung Medical University Hospital, No. 100 Tz-You First Road, Kaohsiung 807, Taiwan, [#]Department of Obstetrics and Gynecology, Kaohsiung Medical University Hospital, No. 100 Tz-You First Road, Kaohsiung 807, Taiwan, [⊥]Center of Excellence for Environmental Medicine, Kaohsiung Medical University, No. 100 Shih-Chuan First Road, Kaohsiung 807, Taiwan, and [⊗]Department of Medical Research, Kaohsiung Medical University Hospital, No. 100 Tz-You First Road, Kaohsiung 807, Taiwan

This study is the first to investigate the anticancer effect of tricetin (TCN) in two human liver cancer cell lines, Hep G2 and PLC/PRF/5. TCN induced cancer cell death treatment by triggering mitochondrial and death receptor 5 (DR5) apoptotic pathways. Exposure of Hep G2 and PLC/PRF/5 cells to TCN resulted in cellular glutathione reduction and ROS generation, accompanied by JNK activation and apoptosis. Both of the antioxidants vitamin C and catalase significantly decreased apoptosis by inhibiting the phosphorylation of JNK and subsequently triggering DR5 cell death pathways. The reduction of JNK expression by siRNA decreased TCN-mediated Bim cleavage, DR5 up-regulation, and apoptosis. Furthermore, daily TCN intraperitoneal injections in nude mice with PLC/PRF/5 subcutaneous tumors resulted in an approximately 60% decrease of mean tumor volume, compared with vehicle-treated controls. Taken together, the results of the present study indicate that TCN-induced cell death in liver cancer cells is initiated by ROS generation and that both intrinsic and extrinsic apoptotic pathways contribute to the cell death caused by this highly promising cancer chemopreventive agent.

**KEYWORDS: Tricetin; apoptosis; ROS; JNK; liver cancer**

## INTRODUCTION

Hepatocellular carcinoma (HCC) is one of the most common causes of cancer mortality, responsible for >600 000 deaths annually. The majority of HCC patients die within 7−8 months of the date of diagnosis (*1*). Chronic infection with hepatitis B virus is the predominant risk factor for HCC in Southeast Asia and Africa, and chronic infection with hepatitis C virus is the predominant risk factor for HCC in Western and European countries (*1*, *2*). This pathology is currently controlled by surgery, transplantation, percutaneous ethanol injection, and radiotherapy and is frequently supported by adjuvant chemotherapies (*1*). However, HCC is highly resistant to chemotherapy, and there is still no effective cure for patients with advanced stages of the disease (*3*). Effective chemopreventive treatment for liver cancer would have a tremendous impact on liver cancer morbidity and mortality rates.

All aerobic organisms are subject to physiological oxidant stress as a consequence of aerobic metabolism. Aerobic respiration coupled to the generation of ATP leads to the formation of the superoxide anion radical ($O_2^{\bullet -}$). Superoxide anion radicals can then form other reactive oxygen species (ROS), such as hydrogen peroxide ($H_2O_2$) and the highly reactive hydroxyl radical ($^{\bullet}OH$) (*4*). The redox status of all aerobic cells is balanced by enzyme and nonenzyme systems (*4*, *5*). Oxidative stress occurs when this critical balance is disrupted because of excess ROS production and/or antioxidant depletion (*5*). Evidence is accumulating which indicates that many chemotherapeutic agents may be selectively toxic to tumor cells because they increase oxidant stress and enhance these already stressed cells beyond their limit (*6*−*8*). Cytotoxic ROS signaling appears to be triggered by the activation of the mitochondrial-dependent cell death pathway through activation of the mitogen-activated protein kinase (MAPK) pathways and the proapoptotic Bcl-2 proteins Bax or Bak, with subsequent mitochondrial membrane permeabilization and cell death (*7*, *8*).

Tricetin (5,7,3′,4′,5′-pentahydroxyflavone) (TCN; **Figure 1A**), a flavonoid derivative found in Myrtaceae pollen and *Eucalyptus* honey (*9*−*11*), has potent antiinflammatory and anticancer activities (*12*, *13*). This study is the first to determine the cell growth inhibition activity of TCN in two HCC tumor cell lines, a

*Author to whom correspondence should be addressed (phone +886-7-312-1101, ext. 5528; fax +886-7-321-0701; e-mail kuopolin@seed.net.tw).


Published on Web 11/10/2010

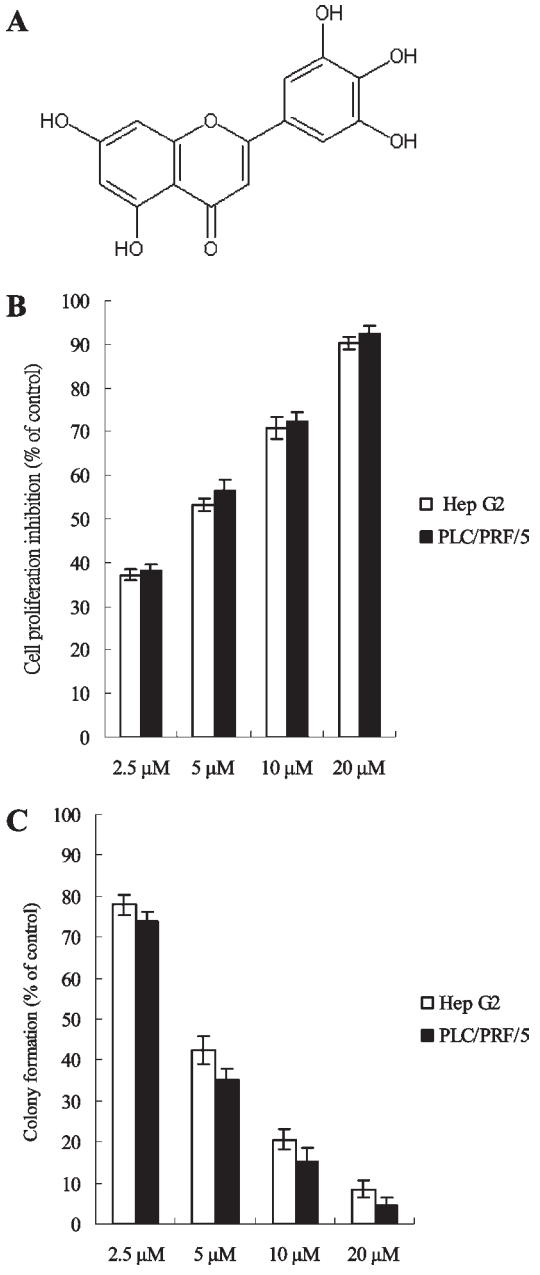


**Figure 1.** Effects of TCN on cell proliferative inhibition and colony formation in liver cancer cell lines Hep G2 and PLC/PRF/5: (**A**) chemical structure of TCN; (**B**) cell proliferative inhibition effect of TCN in Hep G2 and PLC/PRF/5; (**C**) influence of Hep G2 and PLC/PRF/5 on the number of colony-forming cells, as evaluated by clonogenic assay. Cell growth inhibition activity of TCN was assessed by XTT. For the colony-forming assay, the clonogenic assay was performed as described under Materials and Methods. Results are expressed as the percentage of cell proliferation relative to the proliferation of control. The data shown are the mean from three independent experiments. Each value is the mean ± SD of three determinations.

poorly differentiated PLC/PRF/5 cell line (p53 mutant, K-Ras mutant, hepatitis B virus integration) and a well-differentiated Hep G2 (p53 wild type, K-Ras mutant, lacking the hepatitis B virus integration). Our data have found that TCN increases the level of ROS in the human liver cancer cells, and this increase is responsible for its apoptotic effects. TCN-induced ROS activated JNK and subsequently triggered mitochondrial and DR5 apoptotic pathways. Also, TCN's anticancer activity was further examined in a xenografts model. On the other hand, TCN did not exhibit any toxicity in the nude mice's body weight and organs. These data suggest that TCN may be of value in the development of novel therapeutic approaches for the treatment of liver cancer.

## MATERIALS AND METHODS

**Reagents and Cell Culture.** Human hepatocellular carcinoma cell lines Hep G2 (ATCC HB8065) and PLC/PRF/5 (ATCC CRL 8024) were obtained from the American Type Cell Culture Collection (Manassas, VA). Hep G2 and PLC/PRF/5 cells were maintained in monolayer cultures at 37 °C and 5% $CO_2$ in DMEM (Invitrogen, Carlsbad, CA) supplemented with 10% FCS, 10 U/mL penicillin, 10 $\mu$g/mL streptomycin, and 0.25 $\mu$g/mL amphotericin B (GIBCO, Gaithersburg, MD). TCN was purchased from Extrasynthese (Genay, France), dissolved in DMSO (Sigma Aldrich, St. Louis, MO), and stored at −20 °C. For all experiments, the final concentrations of the test compound were prepared by diluting the stock with DMEM. Control cultures received the carrier solvent (0.1% DMSO).

**Cell Proliferation and Clonogenic Assay.** Inhibition of cell proliferation by tricetin was measured by XTT (sodium 3′-[1-(phenylaminocarbonyl)-3,4-tetrazolium]bis(4-methoxy-6-nitro)benzenesulfonic acid hydrate) assay. Briefly, cells were plated in 96-well culture plates ($1 \times 10^4$ cells/well) and, after 24 h of incubation, treated with vehicle alone (0.1% DMSO) and various concentrations of tricetin for 48 h. One hundred and fifty microliters of XTT test solution, which was prepared by mixing 5 mL of XTT-labeling reagent with 100 $\mu$L of electron-coupling reagent, was then added to each well. After 4 h of incubation, absorbance was measured on an ELISA reader (Multiskan EX, Labsystems) at a test wavelength of 492 nm and a reference wavelength of 690 nm.

To determine long-term effects, cells were treated with TCN at various concentrations for 1 h. After being rinsed with fresh medium, cells were allowed to form colonies for 14 days, which were then stained with crystal violet (0.4 g/L; Sigma).

**Apoptosis Assay.** Quantitative assessment of apoptotic cells was assessed by the terminal deoxynucleotidyl transferase-mediated deoxyuridine triphosphate nick end-labeling (TUNEL) method, which examines DNA strand breaks during apoptosis by using a BD ApoAlert DNA Fragmentation Assay kit, as described previously (*14*).

**Immunoblot and JNK Kinase Activity Assays.** Cells were treated with 10 $\mu$M TCN and were lysed on ice for 40 min in a solution containing 50 mM Tris, 1% Triton X-100, 0.1% SDS, 150 mM NaCl, 2 mM $Na_3VO_4$, 2 mM EGTA, 12 mM $\beta$-glycerolphosphate, 10 mM NaF, 16 $\mu$g/mL benzamidine hydrochloride, 10 $\mu$g/mL phenanthroline, 10 $\mu$g/mL aprotinin, 10 $\mu$g/mL leupeptin, 10 $\mu$g/mL pepstatin, and 1 mM phenylmethanesulfonyl fluoride. The cell lysate was centrifuged at 14000*g* for 15 min, and the supernatant fraction was collected for immunoblot. Equivalent amounts of protein were resolved by SDS-PAGE (6−12%) and transferred to PVDF membranes. After blocking for 1 h in 5% nonfat dry milk in Tris-buffered saline, the membrane was incubated with the desired primary antibody for 1−16 h. The membrane was then treated with the appropriate peroxidase-conjugated secondary antibody, and the immunoreactive proteins were detected using an enhanced chemiluminescence kit (Amersham, USA) according to the manufacturer's instructions. The JNK MAPK activities were determined using kits from Cell Signaling Technology (Beverly, MA) according to the manufacturer's instructions.

**Flow Cytometric Analysis of Death Receptors.** Cells were analyzed for the surface expression of DR5 receptor by indirect staining with primary goat anti-human DR5 antibodies (R&D Systems), followed by FITC-conjugated rabbit anti-goat IgG. Briefly, cells were stained with 200 $\mu$L of PBS containing saturated amounts of anti-DR5 antibody for 30 min at 4 °C. After incubation, cells were washed twice and reacted with FITC-conjugated rabbit anti-goat IgG for 30 min at 4 °C. After washing with PBS, the expressions of these death receptors were analyzed by a flow cytometer (Becton Dickinson and Co., Franklin Lakes, NJ).

**Mitochondrial Membrane Potential Assay.** We used mitochondrial-specific cationic dye JC-1 (5,5′,6,6′-tetrachloro-1,1′,3,3′- tetraethylbenzimidazolylcarbocyanine iodide) (Molecular Probes, Inc.), which undergoes potential-dependent accumulation in the mitochondria. It is a monomer when the membrane potential ($\Delta\Psi_m$) is lower than 120 mV and emits a green light (540 nm) following excitation by blue light (490 nm). At higher membrane potentials, JC-1 monomers convert to J-aggregates that

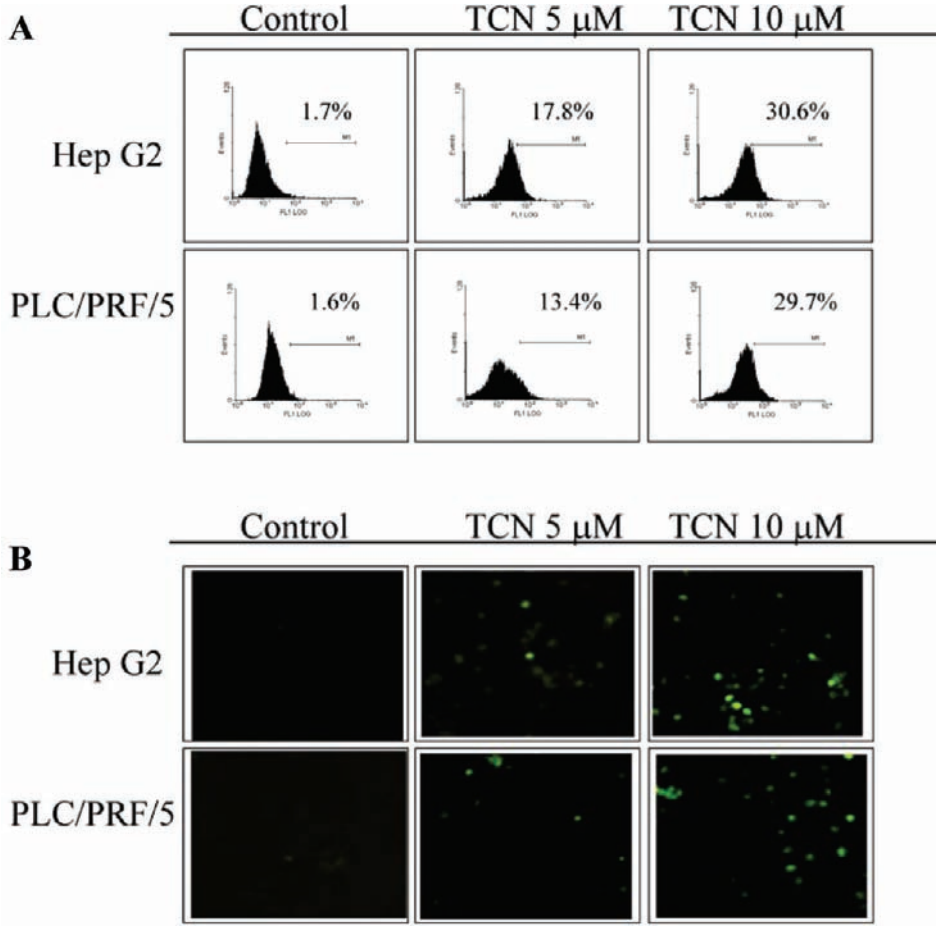


**Figure 2.** Effect of TCN on the induction of apoptosis in Hep G2 and PLC/PRF/5 cells: quantitative evaluations of TUNEL assay by (**A**) flow cytometry and (**B**) fluorescent microscope. TUNEL-positive cells were examined by flow cytometry and were visible through fluorescent microscope. Each value is the mean ± SD of three determinations.

emit a red light (590 nm) following excitation by green light (540 nm). Cells were seeded in a 96-well plate. Following treatment with various concentrations of TCN for the indicated times, cells were stained with 25 $\mu$M JC-1 for 30 min at 37 °C. Fluorescence was monitored with the fluorescence plate reader at wavelength pairs of 490 nm (excitation)/540 nm (emission) and 540 nm (excitation)/590 nm (emission). Changes in the ratio between the measurement at test wavelengths of 590 nm (red) and 540 nm (green) fluorescence intensities are indicative of changes in the mitochondrial membrane potential.

**Assay for Caspase-9 and Caspase-8 Activities.** The assay is based on the ability of the active enzyme to cleave the chromophore from the enzyme substrate: Ac-IETD-pNA (Ac-Ile-Glu-Thr-Asp-*p*NA) for caspase-8 and LEHD-pNA (Ac-Leu-Glu-His-Asp-*p*NA) for caspase-9. Cell lysates were incubated with peptide substrate in assay buffer (100 mM NaCl, 50 mM HEPES, 10 mM dithiothreitol, 1 mM EDTA, 10% glycerol, 0.1% CHAPS, pH 7.4) for 2 h at 37 °C. The release of *p*-nitroaniline was monitored at 405 nm. Results are represented as the percentage of change of activity compared to the untreated control.

**Measurements of ROS and Glutathione.** Cells were plated at a density of $5 \times 10^5$ or $1 \times 10^6$, respectively, in 60 mm dishes, allowed to attach overnight, and exposed to catalase (1000 units/mL) alone, vitamin C (100 $\mu$M) alone, TCN (10 $\mu$M) alone, catalase plus TCN, or vitamin C plus TCN for specified time intervals. The cells were stained with 10 $\mu$M $H_2$DCFDA (for ROS) and CMFDA (for glutathione) for 10 min at 37 °C, and the fluorescence intensity of the cells was determined by flow cytometer (Becton Dickinson and Co.).

**siRNA-Based Knockdown of JNK and DR5 Expression.** Liver cancer cell monolayers were transfected with JNK siRNA expression plasmid pKD-JNK1α1/SAPK1c-v4 or pKD-NegCon-v1 (Upstate Biotechnology Inc., Laker Placid, NY) by using Lipofectamine 2000 (Invitrogen). The inhibition of DR5 expression was performed by DR5 siRNA transfection (Santa Cruz Biotechnology, Santa Cruz, CA). Immunoblot analyses showed that JNK remained low but detectable and that expression of $\beta$-actin was unaffected by plasmid or siRNA transfection.

**In Vivo Tumor Xenograft Experiments.** Male nude mice [6 weeks old; BALB/cA-nu (nu/nu)] were purchased from the National Science Council Animal Center (Taipei, Taiwan) and maintained in pathogen-free conditions. PLC/PRF/5 cells were injected subcutaneously (sc) into the flanks of these nude mice ($5 \times 10^6$ cells in 200 $\mu$L), and tumors were allowed to develop for ~15 days until they reached a size of approximately 100 $mm^3$, when treatment was initiated (*15*). Thirty mice were randomly divided into two groups. The mice in the DHE-treated group were intraperitoneally (ip) injected daily with TCN in a clear solution containing 25% polyethylene glycol (4 mg/kg of body weight), in a volume of 0.2 mL. The control group was treated with an equal volume of vehicle. After transplantation, tumor size was measured using calipers, and tumor volume was estimated according to the following formula: tumor volume ($mm^3$) = $L \times W^2/2$, where $L$ is the length and $W$ is the width. Tumor-bearing mice were sacrificed at 45 days after dosing.

**Statistical Analysis.** Data were expressed as mean ± SD. Statistical comparisons of the results were made using analysis of variance (one-way ANOVA). Statistical analyses of differences between the means of the control and test groups in inhibitor pretreatment and siRNA transfection experiments were based on two-way ANOVAs. Significant differences ($P < 0.05$) between the means of the control and test groups were analyzed by Dunnett's test or Tukey's test (for dose-response effects).

## RESULTS

**TCN Inhibits Cell Proliferation and Clonogenic Survival in both Hep G2 and PLC/PRF/5 Cell Lines.** To investigate the potential cell proliferative inhibition activity of TCN in liver cancer, we first

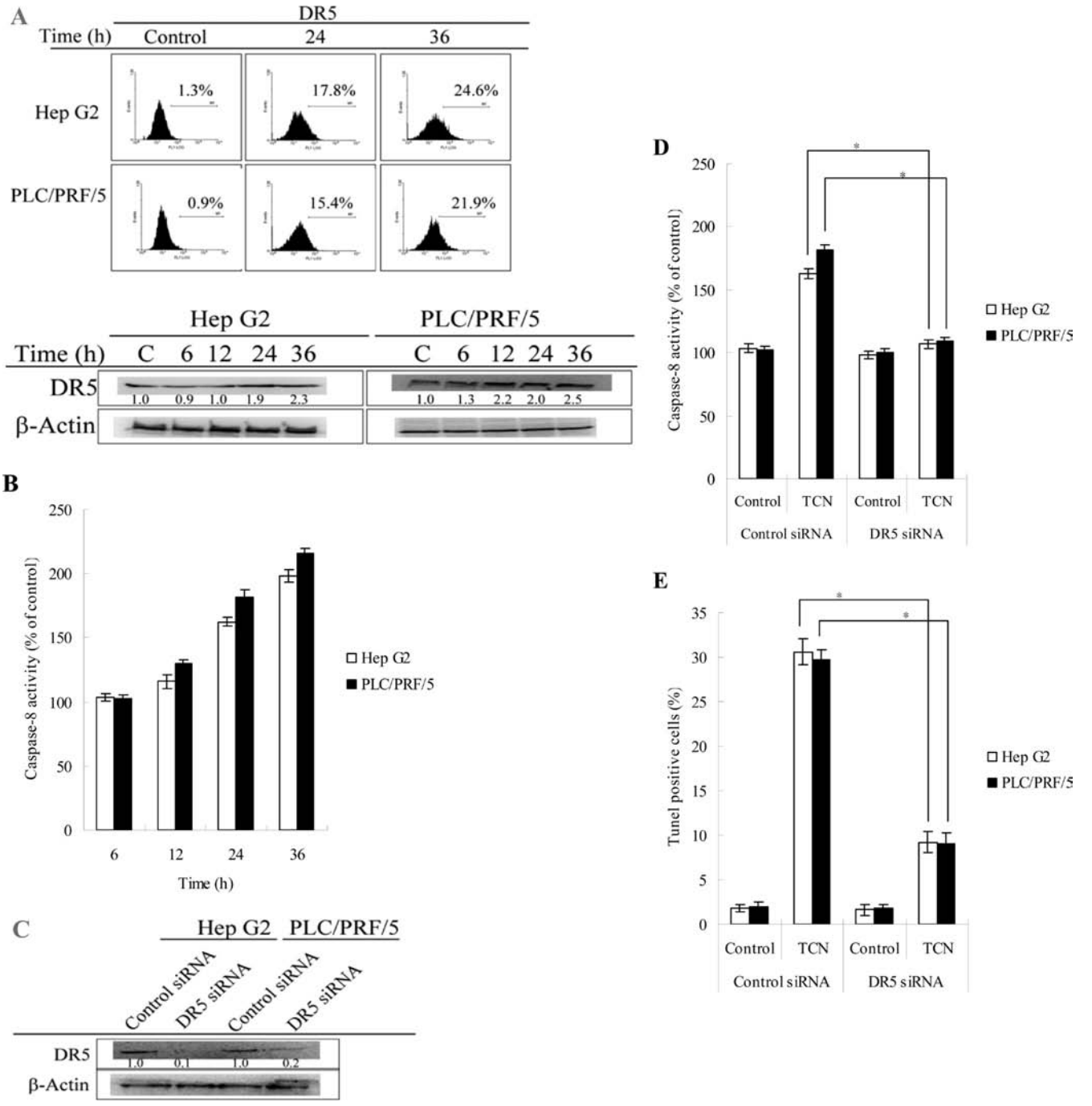


**Figure 3.** TCN-induced death receptor apoptotic pathway. (**A**) TCN increased the expression of DR5. (**B**) TCN induced the activation of caspase-8. (**C**) Genetic suppression of DR5 was accomplished by DR5 siRNA transfection. (**D**) Inhibition of DR5 decreased the activation of caspase-8. (**E**) Inhibition of DR5 decreased TCN-induced apoptosis. Cells were treated with 10 $\mu$M TCN for the indicated times. The expressions of DR5 was assessed by flow cytometry and immunoblot assay. Caspase-8 activity was measured by caspase-8 activity assay kit. For DR5 inhibition, cells were transfected with control siRNA or DR5 siRNA by lipofectamine 2000 agents and then treated with TCN for the indicated times (24 h for caspase-8 activation and 48 h for apoptosis assay). Each value is the mean $\pm$ SD of three determinations. The asterisk indicates a significant difference between two test groups, as analyzed by two-way ANOVA with Dunnett's test post hoc ($p < 0.05$).

examined the effect of TCN on cell proliferation and clonogenic survival in both Hep G2 and PLC/PRF/5 cell lines. As shown in **Figure 1B**, exposure of Hep G2 and PLC/PRF/5 to TCN for 48 h inhibited the growth of each cell line in a dose-dependent manner. The $IC_{50}$ values of TCN were 4.87 $\mu$M for Hep G2 and 4.23 $\mu$M for PLC/PRF/5.

The anticancer activities of TCN inhibition were assessed by clonogenic assays, which correlate very well with in vivo assays of tumorigenicity in nude mice (*16*). Both Hep G2 and PLC/PRF/5 cell lines showed the ability to form clones in the untreated control wells. However, upon the addition of TCN a dose-dependent inhibition in clonogenicity was observed, with a > 50% inhibition at dosages as low as 5 $\mu$M TCN (**Figure 1C**).

**TCN Induces Apoptosis in Human Liver Cancer Cell Lines.** To investigate the mechanisms leading to loss of cell proliferation by TCN, we tested whether the observed inhibition effects of TCN on cell proliferation are due to induction of apoptosis. A quantitative evaluation was made using TUNEL to detect DNA

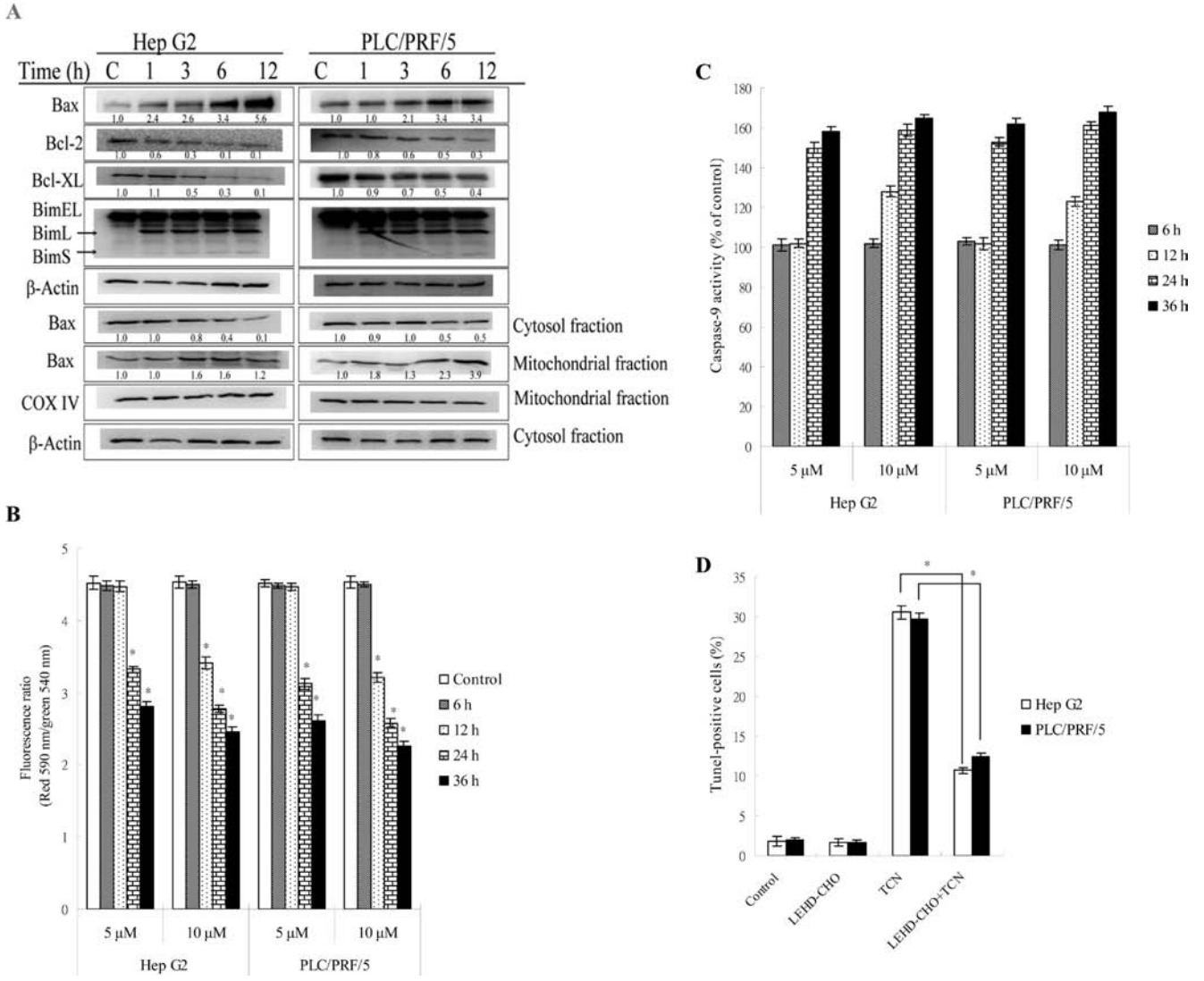


**Figure 4.** TCN triggers mitochondrial pathways: (**A**) effect of TCN on Bcl-2 family proteins and Bax translocation; (**B**) loss of $\Delta\Psi 3_m$; (**C**) activation of caspase-9; (**D**) effect of caspase-9 inhibitor on TCN-induced apoptosis. The levels of Bcl-2 family proteins were assessed by immunoblot assay. $\Delta\Psi_m$ was measured by JC-1 staining. Caspase-9 activity was measured by caspase-9 activity assay kit. For caspase-9 inhibitor blocking experiments, cells were preincubated with LEHD-CHO (20 $\mu$M) for 1 h before the addition of 10 $\mu$M TCN for an additional 48 h. COX IV is the loading control of mitochondrial fraction in immunoblot. Each value is the mean $\pm$ SD of three determinations. The asterisk indicates a significant difference between two test groups, as analyzed by two-way ANOVA with Dunnett's test post hoc ($p < 0.05$).

strand breaks. Compared to vehicle-treated cells, 10 $\mu$M TCN induced apoptosis in 30.6% of the Hep G2 and 29.7% of the PLC/PRF/5 cells at 48 h (**Figure 2A**). TUNEL-positive cells were also examined using a fluorescent microscope (**Figure 2B**).

**DR5 Is Involved in TCN-Mediated Apoptosis.** To establish the sequence of events occurring during TCN-induced apoptosis, we measured some of the molecular activity of the death receptor apoptotic pathway, including DR5. TCN treatment increased DR5 levels in both cancer cell lines, with maximum levels of DR5 detected at 36 h (**Figure 3A**). We next measured the downstream caspase of the DR5 system. The results showed that caspase-8 activity reached maximum induction at 36 h in TCN-treated Hep G2 and PLC/PRF/5 cells (**Figure 3B**).

DR5 has been shown to induce apoptotic cell death through caspase-8 activation (*17*). To confirm the central role of DR5 as a key activator of TCN-mediated caspase-8 activation and apoptosis, we transfected Hep G2 and PLC/PRF/5 with DR5 siRNA targeting DR5. As shown in **Figure 3C**, DR5 siRNA reduced DR5 expression in comparison with control siRNA. Selective genetic inhibition of DR5 abrogated TCN-induced caspase-8 activation (**Figure 3D**). Specific knockdown DR5 expression by DR5 siRNA also inhibited TCN-mediated apoptosis (**Figure 3E**). These data clearly indicate that the up-regulation of DR5 might act upstream of caspase-8 and play a key role in TCN-induced apoptosis.

**TCN Induces Mitochondrial Apoptotic Pathway.** The mitochondrial pathway plays a central role in apoptosis. To determine whether TCN induces apoptosis by triggering the mitochondrial apoptotic pathway, we measured the changes of mitochondrial membrane potential ($\Delta\Psi_m$), the activation of the caspase, and the expression of the Bcl-2 family protein (*17*). Immunoblot analysis showed that treatment of Hep G2 and PLC/PRF/5 cells with TCN increased Bax protein levels (**Figure 4A**). TCN also slightly enhanced the levels of three isoforms of BH3-only Bim protein, including BimEL, BimL, and BimS. The TCN-induced changes in BimL protein expression were more pronounced than for BimEL proteins in both cancer cell lines. In contrast, TCN decreased Bcl-2 and Bcl-XL levels, which led to an increase in the proapoptotic/antiapoptotic Bcl-2 ratio (**Figure 4A**). The proapoptotic molecule Bax has been demonstrated to migrate from

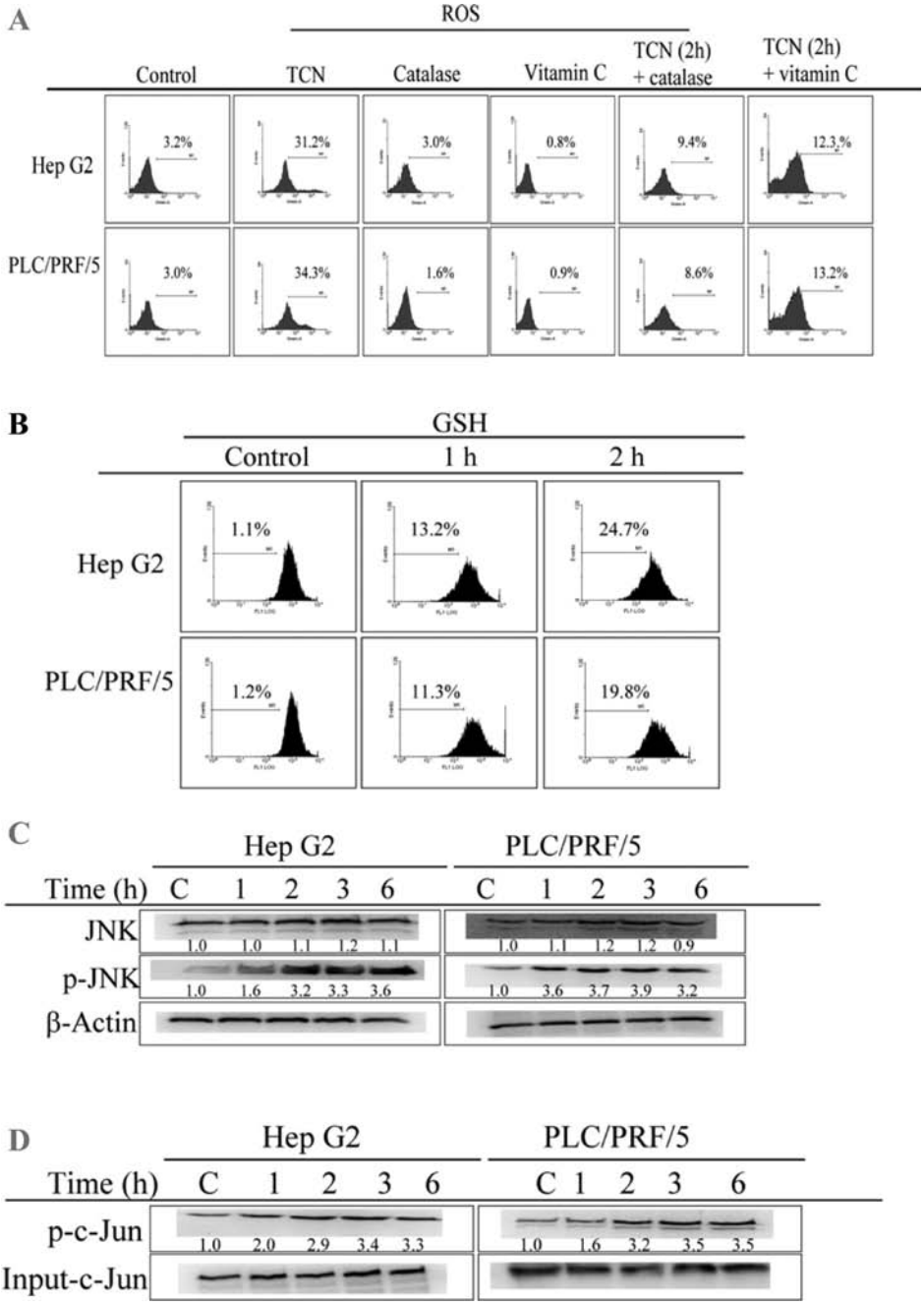


**Figure 5.** Effect of TCN on the production of ROS, the levels of glutathione, and the activation of JNK. (**A**) TCN increased the generation of ROS in Hep G2 and PLC/PRF/5 cells. (**B**) TCN decreased the levels of glutathione. TCN increased the JNK activation (**C**) and activity (**D**) in Hep G2 and PLC/PRF/5 cells. Cells were treated with 10 $\mu$M TCN with or without catalase (1000 units/mL) and vitamin C (100 $\mu$M) for the indicated times, and the amounts of ROS and glutathione were assayed by $H_2$DCFDA (for ROS) and CMFDA (for glutathione) staining. The activation of JNK was assessed by immunoblot assay. JNK kinase activity was determined using a JNK Activity kit from Cell Signaling Technology (Beverly, MA) according to the manufacturer's instructions.

the cytosol to the mitochondria in response to multiple apoptotic stimuli. We therefore examined whether TCN changes localization of Bax protein in Hep G2 and PLC/PRF/5 cells. The subcellular fractionation method showed that Bax protein did indeed move from the cytosol to the mitochondria in both TCN-treated cancer cell lines at 6 h (**Figure 4A**).

We also investigated mitochondrial dysfunction by measuring $\Delta\Psi_m$ in TCN-treated Hep G2 and PLC/PRF/5 cells (**Figure 4B**). Hallmarks of the apoptotic process include the activation of cysteine proteases, which represent both initiators and executors of cell death (*17*). Upstream caspase-9 activities increased significantly, as shown by the observation that treatment with TCN increased caspase-9 activity in both Hep G2 and PLC/PRF/5 cells (**Figure 4C**). Furthermore, when cells were pretreated with the specific caspase-9 inhibitor LEHD-CHO before TCN treatment, the apoptosis induction effect of TCN decreased in both Hep G2 and PLC/PRF/5 cells (**Figure 4D**).

**TCN Increases ROS Production, Decreases Glutathione Levels, and Activates JNK.** Because ROS generation plays an important role in the proapoptotic activities of various anticancer agents (*6*, *7*), we investigated whether ROS generation was required in TCN-induced apoptosis. Intracellular ROS generation in control and TCN-treated Hep G2 and PLC/PRF/5 cells was assessed by flow cytometry following staining with $H_2$DCFDA. TCN treatment exhibited a time-dependent increase in mean DCF fluorescence when compared with control cells in both liver cancer cell

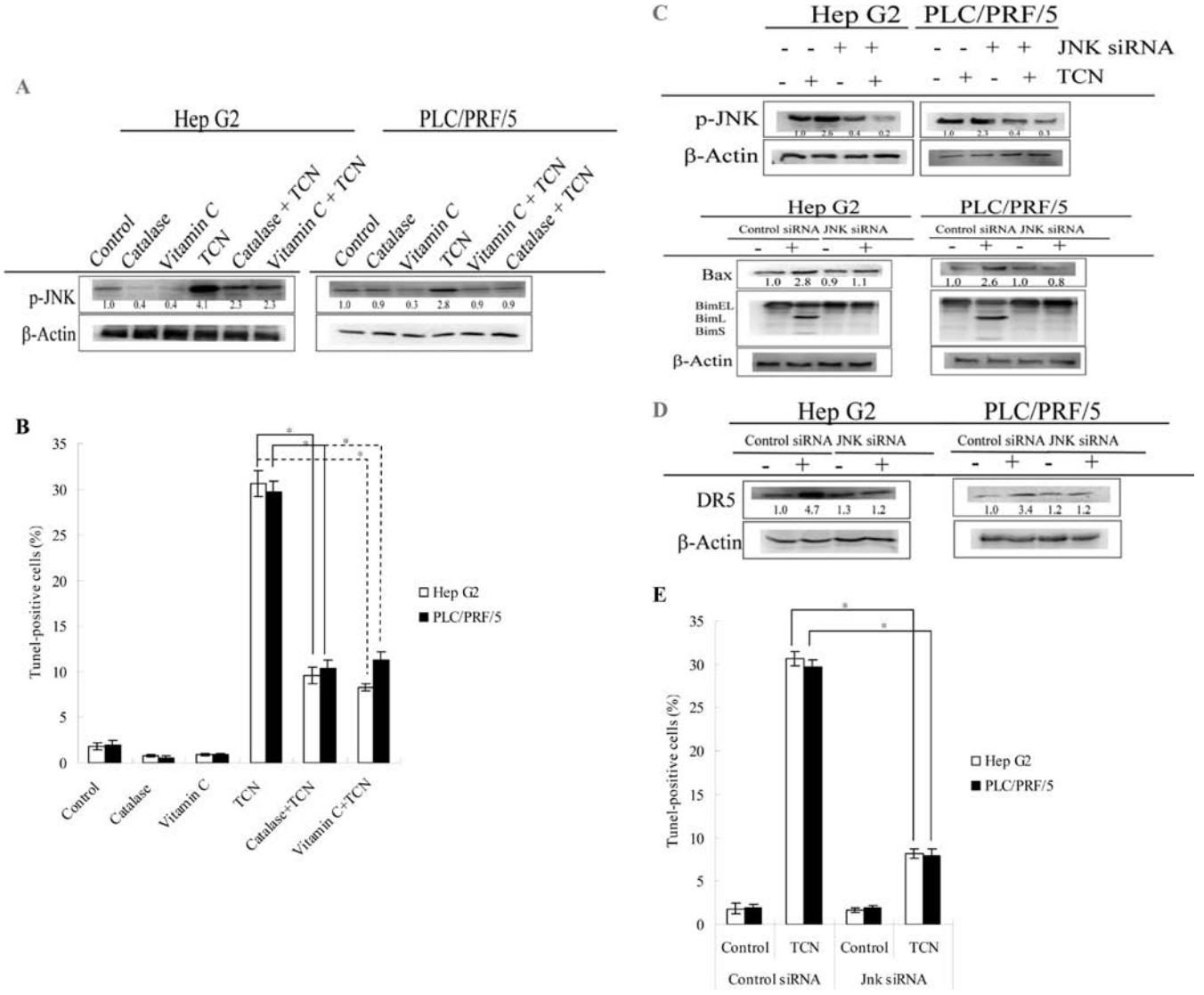


**Figure 6.** Role of ROS and JNK on TCN-mediated apoptosis. Antioxidant agents inhibited TCN-mediated JNK activation (**A**) and apoptosis (**B**). (**C**) Effect of JNK siRNA transfection on the expression of JNK. Inhibition of JNK decreased the enhancement of Bax (**C**), up-regulation of DR5 (**D**), and apoptosis (**E**). For **A** and **B**, cells were pretreated with catalase (1000 units/mL) and vitamin C (100 $\mu$M) for 1 h, and then 10 $\mu$M TCN was added followed by incubation for specific times (3 h for JNK activity and 48 h for apoptosis assay). For **C**−**E**, cells were transfected control or JNK siRNA by liopofectamine 2000 and then incubated with 10 $\mu$M TCN for specific times (12 h for Bax and Bim expression, 36 h for DR5 expression, and 48 h for cell death). The activation of JNK was measured as described in the legend of **Figure 5**. The expression of DR5 was assessed by flow cytometry. The induction of apoptosis was determined by TUNEL analysis. Each value is the mean ± SD of three determinations. The asterisk indicates a significant difference between two test groups, as analyzed by two-way ANOVA with Dunnett's test post hoc ($p < 0.05$).

lines (**Figure 5A**). In addition, two antioxidants, catalase and vitamin C, could prevent the enhancement of ROS caused by TCN. We next investigated whether the generation of ROS induced by the TCN treatment is accompanied by the loss of glutathione, a thiol antioxidant against oxidant stress. The result showed that TCN treatment also decreased glutathione levels in both cancer cell lines after 1 h of exposure (**Figure 5B**).

Because it has been shown that the ROS-mediated DNA damage triggers activation of JNK and subsequent cell death, we assessed the status of JNK phosphorylation after TCN treatment (*7*). **Figure 5C** shows that activation (phosphorylation) of JNK was evident as early as 1 h after TCN treatment and persisted for the duration of the experiment. On the other hand, the expression of JNK (unphosphorylated form) was not affected by TCN treatment. TCN-mediated activation of JNK was further confirmed by determining the phosphorylation of one of its substrates, c-Jun. As shown in **Figure 5D**, in comparison with the control, the Ser63 phosphorylation of c-Jun increased after Hep G2 and PLC/PRF/5 cells were exposed to 10 $\mu$M TCN. Phosphorylation of c-Jun increased relative to the control (**Figure 5D**).

**Antioxidant Protected against TCN-Induced JNK Activation and Cell Death in Hep G2 and PLC/PRF/5 Cells.** A previous study has reported that ROS production induces apoptotic cell death by JNK activation (*7*), thus raising the question of whether production of cellular ROS contributed to TCN-mediated JNK activation and apoptosis. We addressed this possibility by determining the effects of antioxidants on JNK activation and cell death caused by TCN. As shown in **Figure 6A**, pretreatment of Hep G2 and PLC/PRF/5 cells with catalase and vitamin C could prevent the phosphorylation of JNK caused by TCN (**Figure 6A**). We further assessed the effect of antioxidant agents in TCN-induced apoptosis. The results showed that TCN-induced apoptosis in both cancer cell lines was significantly attenuated in catalase- or

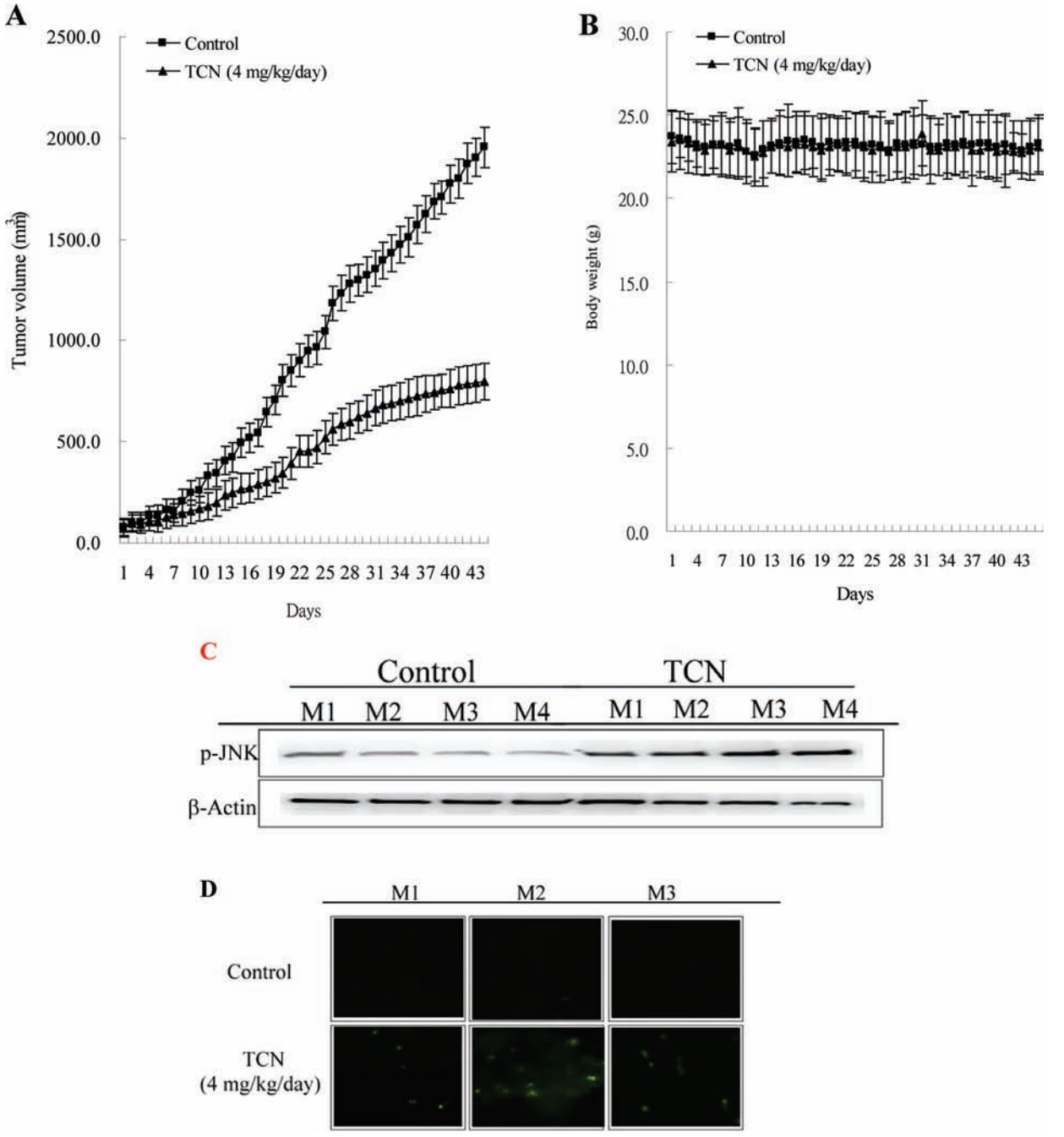


**Figure 7.** TCN inhibits growth of PLC/PRF/5 in nude mice: (**A**) mean of tumor volume measured at the indicated number of days after implant; (**B**) mean of body weight in TCN-treated mice. TCN increased JNK activation (**C**) and induced apoptotic cell death (**D**) in PLC/PRF/5 xenografts. Animals bearing pre-established tumors ($n$ = 15 per group) were dosed daily for 45 days with ip injections of TCN (4 mg/kg/day) or vehicle. During the 45 day treatment, tumor volumes were estimated using measurements taken by external calipers ($mm^3$). The levels of JNK and phospho-JNK in nude mice tumor section were assessed by immunoblot analysis. The induction of apoptosis in nude mice tumor section was determined by TUNEL assay. Each value is the mean ± SD of three determinations.

vitamin C-pretreated cells, compared with TCN-treated Hep G2 and PLC/PRF/5 cells (**Figure 6B**). These data strongly suggest that the generation of ROS plays an important role in TCN-induced JNK activation and apoptosis.

Several studies have indicated that JNK can cause apoptosis by a variety of mechanisms, including regulation of Bcl-2 family proteins and initiation of death receptor (*18*). Next, we assessed the role of JNK on TCN-induced apoptosis. To do so, Hep G2 and PLC/PRF/5 cells were transiently transfected with JNK siRNA. Subsequently, the siRNA-transfected cells were exposed to TCN, and then the levels of DR5, Bax, and Bim and the amount of apoptotic cells were determined. Inhibition of phospho-JNK in TCN-treated Hep G2 and PLC/PRF/5 cells that had been transiently transfected with a JNK siRNA plasmid was confirmed by immunoblot, as shown in **Figure 6C**. TCN treatment caused a marked increase in the protein levels of Bax, BimL, BimS, and DR5, and these effects were inhibited in both JNK-siRNA transfected cell lines (**Figure 6C**,**D**). In addition, our data also show that JNK inhibition almost completely abrogated TCN-induced apoptosis in Hep G2 and PLC/PRF/5 cells (**Figure 6E**). These results suggest that apoptosis induction by TCN was due to JNK activation.

**TCN Inhibits Tumor Growth of Human Liver Cancer Xenografts, Associated with JNK Activation and Apoptosis Induction in Vivo.** To determine whether TCN inhibits tumor growth in vivo, equal numbers of PLC/PRF/5 cells were injected subcutaneously into both flanks of the nude mice. Once the tumors reached a palpable size (approximately 100 $mm^3$), the mice were treated daily for 45 days with ip injections of either the vehicle control or 4 mg/kg of TCN. At the end of 45 days, control tumors grew to an average size of $1954 \pm 98.2$ $mm^3$, whereas TCN-treated tumors had grown to $798 \pm 89.3$ $mm^3$. Tumor growth inhibition corresponded to 59.2% growth (**Figure 7A**). Mean body weight (**Figure 7B**) and tissue sections of lungs, livers, and kidneys did not indicate any significant differences between vehicle- and TCN-treated mice (data not shown).

To gain insight into the mechanism of TCN's inhibition of tumor growth in vivo, we harvested the PLC/PRF/5 tumor xenografts from vehicle- and TCN-treated mice. We also extracted proteins to assess levels of phospho-JNK proteins. As shown in **Figure 7D**, an increase of TUNEL-positive cells was observed in the tumors of the TCN-treated mice when compared to tumors taken from vehicle-treated mice. An increase of phospho-JNK was also observed in tumors from the TCN-treated group (**Figure 7C**).

## DISCUSSION

This study is the first to show that TCN, a novel dietary flavonoid from Myrtaceae pollen and *Eucalyptus* honey, inhibits the growth of two human liver cancer cell lines, Hep G2 and PLC/PRF/5, both in vitro and in vivo. Both Hep G2 and PLC/PRF/5 cells treated with TCN underwent apoptosis in a dose-dependent manner.

Death receptor apoptotic pathways have been described as important signals for apoptotic cell death for mammalian cells (*17*). Following the treatment of Hep G2 and PLC/PRF/5 cells with TCN, we observed that TCN treatment increased the expression of DR5. Also, caspase-8 activity was simultaneously enhanced in DR5-up-expressing Hep G2 and PLC/PRF/5. Moreover, selective knockdown DR5 expression by siRNA-based inhibition approach also decreased the effects of TCN on the activation of caspase-8 and apoptosis, suggesting that the cooperation of DR5 plays a crucial role in TCN-induced cell death in human liver cancer cells.

Mitochondria are thought to be another pathway for apoptosis, and mitochondrial function is regulated through Bcl-2 family proteins, composed of both antiapoptotic (Bcl-2, Bcl-XL) and proapoptotic members (Bax, Bak, Bim) (*17*, *19*). The BH3-only Bim has been shown to function as a sensor to apoptotic signals (*19*). BH3-only proteins and BH3 peptides interact with Bax and Bak, resulting in conformational changes, oligomerization, and activation of Bax and Bak to permeabilize the membranes (*19*). Three major isoforms of Bim are generated by alternative splicing: BimEL, BimL, and BimS (*20*). BimS is the most cytotoxic and is generally only transiently expressed during apoptosis (*21*). TCN treatment results in a significant increase of Bax expression and a decrease of Bcl-2 and Bcl-XL, suggesting that changes in the ratio of proapoptotic and antiapoptotic Bcl-2 family proteins might contribute to the apoptosis-promoting activity of TCN. Moreover, TCN-induced up-regulation of BimL and BimS protein appeared to correlate with translocation of Bax, suggesting that Bim expression is closely associated with the activation of Bax. In addition, our findings also showed a collapse of $\Delta\Psi_m$ and activation of caspase-9 after Hep G2 and PLC/PRF/5 cells were treated with TCN. These mitochondrial apoptotic events play an important role in TCN-mediated apoptosis.

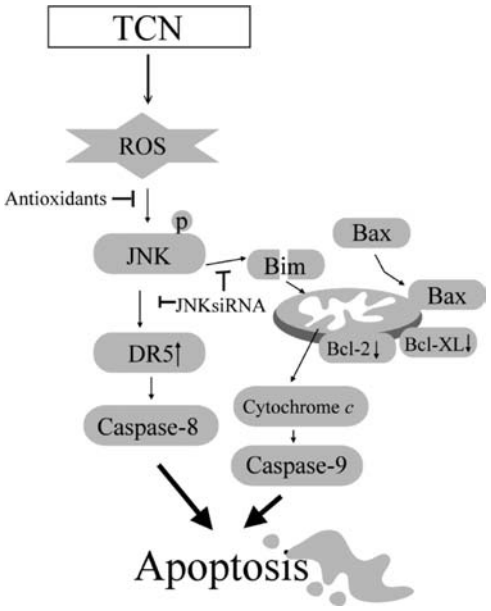


**Figure 8.** Molecular mechanism of TCN-induced apoptosis. TCN caused Hep G2 and PLC/PRF/5 cells to produce ROS, which increased the activation and activity of JNK. The activation of JNK caused an enhanced effect on DR5 and Bax expression as well as Bim cleavage, resulting in apoptosis.

Enhancement of ROS production has long been associated with the apoptotic response induced by several anticancer agents (*7*, *8*, *22*). The status of intracellular redox is regulated by antioxidant enzymes (SOD, catalase, glutathione peroxidase) and nonenzymatic antioxidants (GSH, vitamin C, thioredoxin) (*5*). GSH is a major thiol−disulfide redox buffer that participates in redox reactions by maintaining a reducing environment in the cell. Up-regulation of GSH levels are an important factor in protection against apoptosis and are associated with cancers resistant to therapy (*23*, *24*). Consequently, low GSH levels are sometimes associated with mitochondrial dysfunction and induction of apoptosis, thereby decreasing cancer's chemoresistance (*22*, *25*). ROS can cause apoptotic cell death via a variety of mechanisms, among which the activation of stress kinases JNK plays an important role. Our study showed that TCN-mediated oxidative stress resulted mainly from GSH depletion. We further observed that TCN generates ROS and activates JNK, resulting in caspase-9 activation. Furthermore, these agents can regulate ROS detoxification, such as the scavengers of oxygen-free radicals vitamin C, and the $H_2O_2$-scavenging enzyme catalase, which inhibits JNK activation and decreases apoptosis induced by TCN. These data suggest that ROS accumulation contributes to TCN-induced cell death in human liver cancer cells.

JNKs have been implicated in the apoptotic response of cells exposed to UV irradiation, heat shock, chemotherapy, and proinflammatory cytokines (*25*, *26*). A number of anticancer drugs have been reported to kill liver cancer cells via the JNK apoptotic pathway, so it is to be expected that blockade of JNK activation could inhibit anticancer activity (*27*, *28*). In addition, inhibition of JNK by MKP-1 has been shown to inhibit chemotherapy agent-induced apoptosis (*29*, *30*). The proapoptotic targets of the activated JNK are not clearly defined, but the phosphorylation of transcription factors such as c-Jun and p53, as well as pro- and antiapoptotic Bcl-2 family members such as Bim, Bax, and Bcl-2, have been suggested to be of importance (*25*). In this paper, we have shown that treatment of Hep G2 and PLC/PRF/5 cells with TCN resulted in the accumulation of phospho-JNK in both in vitro and in vivo cancer cells. This JNK activation correlated well with the TCN-induced increase of

JNK activity, as measured by the JNK substrate phospho-c-Jun. Furthermore, we observed that blocking the TCN-induced activation of JNK by JNK siRNA prevents DR5 enhancement, Bim (BimL and BimS) expression, and Bax translocation, suggesting that TCN-induced JNK activation contributes to both TCN-induced death receptor and mitochondrial apoptotic pathways. Moreover, the inhibition of JNK also prevented TCN-induced apoptosis, further suggesting that the cooperation of JNK with DR5 and mitochondrial apoptotic pathway plays a crucial role in TCN-induced apoptosis.

In conclusion, our data indicate that human liver cancer cells are highly sensitive to growth inhibition and apoptosis induction by TCN. TCN-induced apoptosis is associated with mitochondrial and DR5 cell death pathways, which are mediated by ROS generation and, subsequently, JNK activation (**Figure 8**). The proposed working models for the molecular basis, if confirmed, would provide invaluable insights for approaches to the development of effective chemotherapy by targeting appropriate signal transducers.

## LITERATURE CITED


(1) Llovet, J. M.; Burroughs, A.; Bruix, J. Hepatocellular carcinoma. *Lancet* **2003**, *362*, 1907−1917.

(2) El Serag, H. B.; Mason, A. C. Rising incidence of hepatocellular carcinoma in the United States. *N. Engl. J. Med.* **1999**, *340*, 745−750.

(3) Raoul, J. L. Natural history of hepatocellular carcinoma and current treatment options. *Semin. Nucl. Med.* **2008**, *38*, S13−S18.

(4) Fujino, G.; Noguchi, T.; Takeda, K.; Ichijo, H. Thioredoxin and protein kinases in redox signaling. *Semin. Cancer Biol.* **2006**, *16*, 427−435.

(5) Kondo, N.; Nakamura, H.; Masutani, H.; Yodoi, J. Redox regulation of human thioredoxin network. *Antioxid. Redox. Signal.* **2006**, *8*, 1881−1890.

(6) Moungjaroen, J.; Nimmannit, U.; Callery, P. S.; Wang, L.; Azad, N.; Lipipun, V.; Chanvorachote, P.; Rojanasakul, Y. Reactive oxygen species mediate caspase activation and apoptosis induced by lipoic acid in human lung epithelial cancer cells through Bcl-2 down-regulation. *J. Pharmacol. Exp. Ther.* **2006**, *319*, 1062−1069.

(7) Kim, B. C.; Kim, H. G.; Lee, S. A.; Lim, S.; Park, E. H.; Kim, S. J.; Lim, C. J. Genipin-induced apoptosis in hepatoma cells is mediated by reactive oxygenspecies/c-Jun $NH_2$-terminal kinase-dependent activation of mitochondrial pathway. *Biochem. Pharmacol.* **2005**, *70*, 1398−1407.

(8) Kuo, P. L.; Chen, C. Y.; Hsu, Y. L. Isoobtusilactone A induces cell cycle arrest and apoptosis through reactive oxygen species/apoptosis signal-regulating kinase 1 signaling pathway in human breast cancer cells. *Cancer Res.* **2007**, *67*, 7406−7420.

(9) Yao, L.; Jiang, Y.; D′Arcy, B.; Singanusong, R.; Datta, N.; Caffin, N.; Raymont, K. Quantitative high-performance liquid chromatography analyses of flavonoids in Australian Eucalyptus honeys. *J. Agric. Food Chem.* **2004**, *52*, 210−214.

(10) Martos, I.; Ferreres, F.; Yao, L.; D'Arcy, B.; Caffin, N.; Tomás-Barberán, F. A. Flavonoids in monospecific eucalyptus honeys from Australia. *J. Agric. Food Chem.* **2000**, *48*, 4744−4748.

(11) Martos, I.; Ferreres, F.; Tomás-Barberán, F. A. Identification of flavonoid markers for the botanical origin of Eucalyptus honey. *J. Agric. Food Chem.* **2000**, *48*, 1498−1502.

(12) Geraets, L.; Moonen, H. J.; Brauers, K.; Wouters, E. F.; Bast, A.; Hageman, G. J. Dietary flavones and flavonoles are inhibitors of poly(ADP-ribose)polymerase-1 in pulmonary epithelial cells. *J. Nutr.* **2007**, *137*, 2190−2195.

(13) Hsu, Y. L.; Uen, Y. H.; Chen, Y.; Liang, H. L.; Kuo, P. L. Tricetin, a dietary flavonoid, inhibits proliferation of human breast adenocarcinoma mcf-7 cells by blocking cell cycle progression and inducing apoptosis. *J. Agric. Food Chem.* **2009**, *57*, 8688−8695.

(14) Hsu, Y. L.; Kuo, P. L.; Lin, L. T.; Lin, C. C. Asiatic acid, a triterpene, induces apoptosis and cell cycle arrest through activation of extracellular signal-regulated kinase and p38 mitogen-activated protein kinase pathways in human breast cancer cells. *J. Pharmacol. Exp. Ther.* **2005**, *313*, 333−344.

(15) Kuo, P. L.; Hsu, Y. L.; Cho, C. Y. Plumbagin induces G2-M arrest and autophagy by inhibiting the AKT/mammalian target of rapamycin pathway in breast cancer cells. *Mol. Cancer Ther.* **2006**, *5*, 3209−3221.

(16) Freedman, V. H.; Shin, S. I. Cellular tumorigenicity in nude mice: correlation with cell growth in semi-solid medium. *Cell* **1974**, *3*, 355−359.

(17) Hengartner, M. O. The biochemistry of apoptosis. *Nature* **2000**, *407*, 770−776.

(18) Zu, K.; Hawthorn, L.; Ip, C. Up-regulation of c-Jun-NH2-kinase pathway contributes to the induction of mitochondria-mediated apoptosis by alpha-tocopheryl succinate in human prostate cancer cells. *Mol. Cancer Ther.* **2005**, *4*, 43−50.

(19) Labi, V.; Erlacher, M.; Kiessling, S.; Villunger, A. BH3-only proteins in cell death initiation, malignant disease and anticancer therapy. *Cell Death Differ.* **2006**, *13*, 1325−1338.

(20) Bouillet, P.; Zhang, L. C.; Huang, D. C.; Webb, G. C.; Bottema, C. D.; Shore, P.; Eyre, H. J.; Sutherland, G. R.; Adams, J. M. Gene structure alternative splicing, and chromosomal localization of pro-apoptotic Bcl-2 relative Bim. *Mamm. Genome* **2001**, *12*, 163−168.

(21) Yip, K. W.; Li, A.; Li, J. H.; Shi, W.; Chia, M. C.; Rashid, S. A.; Mocanu, J. D.; Louie, A. V.; Sanchez, O.; Huang, D.; Busson, P.; Yeh, W. C.; Gilbert, R.; O'Sullivan, B.; Gullane, P.; Liu, F. F. Potential utility of BimS as a novel apoptotic therapeutic molecule. *Mol. Ther.* **2004**, *10*, 533−544.

(22) Filomeni, G.; Aquilano, K.; Rotilio, G.; Ciriolo, M. R. Glutathione-related systems and modulation of extracellular signal-regulated kinases are involved in the resistance of AGS adenocarcinoma gastric cells to diallyl disulfide-induced apoptosis. *Cancer Res.* **2005**, *65*, 11735−11742.

(23) Wright, S. C.; Wang, H.; Wei, Q. S.; Kinder, D. H.; Larrick, J. W. Bcl-2-mediated resistance to apoptosis is associated with glutathione-induced inhibition of AP24 activation of nuclear DNA fragmentation. *Cancer Res.* **1998**, *58*, 5570−5576.

(24) Ramos, A. M.; Fernandez, C.; Amran, D.; Esteban, D.; de Blas, E.; Palacios, M. A.; Aller, P. Pharmacologic inhibitors of extracellular signal-regulated kinase (ERKs) and c-Jun NH(2)-terminal kinase (JNK) decrease glutathione content and sensitize human promonocytic leukemia cells to arsenic trioxide-induced apoptosis. *J. Cell Physiol.* **2006**, *209*, 1006−1015.

(25) Iwamaru, A.; Iwado, E.; Kondo, S.; Newman, R. A.; Vera, B.; Rodriguez, A. D.; Kondo, Y. Eupalmerin acetate, a novel anticancer agent from Caribbean gorgonian octocorals, induces apoptosis in malignant glioma cells via the c-Jun NH2-terminal kinase pathway. *Mol. Cancer Ther.* **2007**, *6*, 184−192.

(26) Hsu, Y. L.; Cho, C. Y.; Kuo, P. L.; Huang, Y. T.; Lin, C. C. Plumbagin (5-hydroxy-2-methyl-1,4-naphthoquinone) induces apoptosis and cell cycle arrest in A549 cells through p53 accumulation via c-Jun NH2-terminal kinase-mediated phosphorylation at serine 15 in vitro and in vivo. *J. Pharmacol. Exp. Ther.* **2006**, *318*, 484−494.

(27) Lee, H. J.; Wang, C. J.; Kuo, H. C.; Chou, F. P.; Jean, L. F.; Tseng, T. H. Induction apoptosis of luteolin in human hepatoma HepG2 cells involving mitochondria translocation of Bax/Bak and activation of JNK. *Toxicol. Appl. Pharmacol.* **2005**, *203*, 124−131.

(28) Yeh, C.; Yen, G. Induction of apoptosis by the anthocyanidins through regulation of Bcl-2 gene and activation of c-Jun N-terminal kinase cascade in hepatoma cells. *J. Agric. Food Chem.* **2005**, *53*, 1740−1749.

(29) Zhou, J. Y.; Liu, Y.; Wu, G. S. The role of mitogen-activated protein kinase phosphatase-1 in oxidative damage-induced cell death. *Cancer Res.* **2006**, *66*, 4888−4894.

(30) Wu, W.; Pew, T.; Zou, M.; Pang, D.; Conzen, S. D. Glucocorticoid receptor-induced MAPK phosphatase-1 (MPK-1) expression inhibits paclitaxel-associated MAPK activation and contributes to breast cancer cell survival. *J. Biol. Chem.* **2005**, *280*, 4117−4124.


**Received for review August 17, 2010. Revised manuscript received October 10, 2010. Accepted November 1, 2010. This study was supported by grants from the National Science Council of Taiwan (NSC96-2628-B-037-042-MY3), Excellence for Cancer Research Center Grant, Department of Health, Executive Yuan, Taipei, Taiwan (DOH99-TD-C-111-002), Kaohsiung Medical University Hospital (KMUH99-9I04), and Center of Excellence for Environmental Medicine, Kaohsiung Medical University (KMU-EM-98-3).**